PAPER Special Section on Recent Progress in Antennas, Propagation and Wireless Systems Related to Topics in ISAP2014

Channel Capacity Evaluation of MIMO Antenna Based on Eigenvalues of *S*-Parameter

Naoki HONMA[†a)], **Kentaro MURATA**[††], **Hiroshi SATO**[†††], ***Members***, **Koichi OGAWA**[††††], ***Senior Member***, ***and*** **Yoshitaka TSUNEKAWA**[†], ***Member***

SUMMARY In this paper, a method of calculating the mean channel capacity based on *S*-parameter of MIMO (Multiple-Input Multiple-Output) antenna is proposed. This method exploits the correlation matrix calculated from the antenna *S*-parameter matrix, and offers highly accurate estimates of the mean channel capacity without dependence on SNR (Signal-to-Noise Ratio). The numerical and experimental results revealed that the proposed method can calculate the channel capacity with fair accuracy independent of the number and spacing of the antenna elements if the radiation efficiency is sufficiently high.

key words: *MIMO, capacity, S-parameter*

1. Introduction

Evaluating a multiple-input multiple-output (MIMO) antenna is difficult since its radiation patterns and efficiency are not direct indicators of MIMO communication performance [1], [2]. Especially for the terminal MIMO antennas, many antennas need to be built in a small chassis, and this yields several problems with the MIMO communication performance. One problem is strong mutual coupling among antenna elements. The transmitted signal from one of the antennas is captured by other antenna elements and this cause degradation in signal-to-noise ratio (SNR). Indeed, this phenomenon is categorized as the miss-match loss since both the reflected and captured powers go back to the sources. On the basis of the reciprocity of the passive circuit system, this miss-match loss affects the reception performance of the antenna as well. The mutual coupling also causes distortion in the radiation pattern. Even though this affects the spatial correlation coefficient, the spatial correlation is sometimes improved by mutual coupling [1]. As described here, the mutual coupling plays an important role in determining the channel capacity since it strongly affects these two factors, i.e. SNR and spatial correlation.

The spatial correlation characteristics of a MIMO system are determined by both propagation characteristics and complex radiation patterns [3], [4]. The propagation characteristics depend on the various factors, e.g. Rician factor, path distributions, and cross-polarization discrimination in the path. Furthermore, it is significantly affected by the orientation and location of the antennas. Therefore, the deterministic evaluation of the MIMO antenna is quite difficult. On the other hand, the diversity-antenna evaluation method using the simplified path distribution model and complex radiation patterns has been studied [5]–[7]. However, these methods require the 3D-complex radiation patterns for all antenna elements. Although various methods for measuring 3D-complex radiation pattern have been used [8], [9], further simplified and cost effective method is desired.

The antenna characteristics can be recognized to be deterministic since this is determined when the antenna is manufactured if we neglect the effect of the surrounding objects such as the human body. On the other hand, the channel always varies since the orientation and location of the antenna is uncertain in mobile communication system, such as cellular terminals. Therefore, the MIMO antenna evaluation method without depending on the channel characteristics is needed if our interest is limited to the antenna performance. S. Blanch et al. have proposed a simple method for calculating envelope correlation coefficient only from *S*-parameters of the multiple antenna system [10], where the channel is simplified to three-dimensional (3D) uniform. If the ohmic loss in the antennas is negligible, this is quite convenient for evaluating MIMO antenna performance because we do not need to consider the either the propagation environment or complex radiation patterns. However, this method only calculates the correlation coefficients and does not directly translate the antenna characteristics to MIMO channel capacity. For this reason, the capacity-based evaluation of the MIMO antennas is used in many studies [11]–[13].

By extending the idea of [10], the authors have presented a closed-form equation for calculating mean channel capacity of MIMO antenna, where only *S*-parameters and SNR are needed [14], [15]. Thanks to its closed-form expression, Monte Carlo simulations are not needed for evaluating mean channel capacity. Even though this equation is simple and convenient, the accuracy is poor especially at low SNR cases.

In this paper, a fairly accurate channel capacity equation only based on *S*-parameters is proposed. In this equation, the eigenvalues of the *S*-parameter matrix of the MIMO antenna is used. Also, mean eigenvalues of iid (inde-

Manuscript received April 6, 2015.
Manuscript revised August 17, 2015.

[†]The authors are with Iwate University, Morioka-shi, 020-8551 Japan.
[††]The author is with Graduate School of Science and Engineering, National Defense Academy, Yokosuka-shi, 239-8686 Japan.
[†††]The author is with Panasonic System Networks Co., Ltd., Yokohama-shi, 224-8539 Japan.
[††††]The author is with Toyama University, Toyama-shi, 930-8555 Japan.
a) E-mail: honma@m.ieice.org

DOI: 10.1587/transcom.2015ISP0023

Copyright © 2016 The Institute of Electronics, Information and Communication Engineers

pendently and identically distributed) random channel matrices are used. Since the combination of the antennas and propagation characteristics determines the channel capacity, the interaction of them causes uncertainness in capacity calculation. To resolve this problem, the upper and lower capacity bounds are calculated from these eigenvalues, and the average of these two bounds is approximated as the mean channel capacity. This means mean channel capacity can be calculated without Monte Carlo simulations. In the following part of the paper, the derivation of the equation is described. Furthermore, the validity of the proposed equation is evaluated numerically and experimentally.

2. System Model and Proposed Equation

2.1 System Model

Figure 1 shows a conceptual sketch of the multiple antennas and channel model. This model assumes Rayleigh channel, where sufficiently many paths exist around the antennas, and the paths distribute in 3D random directions (3D uniform) [2], [16]. Also, the transmitting antennas are not shown in this model because our interest here is only a set of MIMO array. This model assumes the ideally uncorrelated transmitting antenna array that has antenna elements as many as that of the receiving array. The S-parameter matrix of M element MIMO array is defined as $\boldsymbol{S}_A$ ($\in \mathbb{C}^{M\times M}$). This study assumes the MIMO array is lossless, i.e. it may have the mismatch loss and mutual couplings but does not have ohmic loss because this paper uses the approximation of [10] for calculating the correlation matrix.

2.2 Mean Channel Capacity Based on Eigenvalues of S-Parameter

The 3D complex radiation pattern of i-th antenna is defined as,

$$\boldsymbol{D}_i(\theta,\phi) = [D_{\theta i}(\theta,\phi), D_{\phi i}(\theta,\phi)]^T. \tag{1}$$

The correlation matrix of the MIMO array is calculated by the radiation integral of the product of the complex patterns as,

$$\boldsymbol{R}_A = \frac{1}{4\pi}\int\int \begin{bmatrix} \boldsymbol{D}_1^H\boldsymbol{D}_1 & \cdots & \boldsymbol{D}_1^H\boldsymbol{D}_M \\ \vdots & \ddots & \vdots \\ \boldsymbol{D}_M^H\boldsymbol{D}_1 & \cdots & \boldsymbol{D}_M^H\boldsymbol{D}_M \end{bmatrix} d\Omega. \tag{2}$$

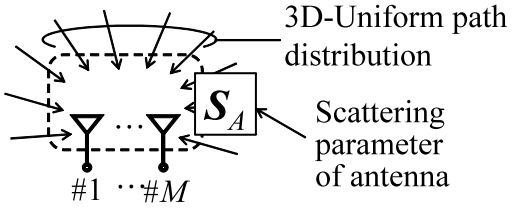

Fig. 1 Conceptual sketch of antennas and channel model.

When the antenna array is lossless, (2) can be simply calculated by

$$\boldsymbol{R}_A = \boldsymbol{I} - \boldsymbol{S}_A^H\boldsymbol{S}_A \tag{3}$$

where $\boldsymbol{I}$ is identity matrix [10].

In Kronecker model, the MIMO channel for this MIMO array can be generated by

$$\boldsymbol{H} = \boldsymbol{R}_A^{1/2}\boldsymbol{H}_W. \tag{4}$$

$\boldsymbol{H}_W$ is $M\times M$ iid channel matrix, where the its elements are zero-mean complex Gaussian random. Figure 2 represents the block diagram of the channel expressed by (4). Because the ideally uncorrelated array is assumed at the transmitter side, the correlation matrix for the transmitting array is expressed by $M\times M$ identity matrix, $\boldsymbol{I}$. For this antenna system, the instantaneous MIMO channel capacity is expressed by,

$$C = \log_2\left|\boldsymbol{H}\boldsymbol{H}^H\frac{\gamma}{M} + \boldsymbol{I}\right| \tag{5}$$

$$= \log_2\left|\boldsymbol{R}_A^{1/2}\boldsymbol{H}_W\boldsymbol{H}_W^H\boldsymbol{R}_A^{1/2H}\frac{\gamma}{M} + \boldsymbol{I}\right| \tag{6}$$

where γ is SNR. Note that the γ is not given value but the parameter we determine. The definition of γ in this paper is the ratio of the signal to the noise when the lossless omnidirectional antennas are used at both the transmitting and receiving sides. This means the actual SNR is different from the determined γ because of the mismatch loss, and so on. Since all of the matrices in (6) are $M\times M$ square, (6) can be re-written as,

$$C = \log_2\left|\boldsymbol{R}_A\boldsymbol{H}_W\boldsymbol{H}_W^H\frac{\gamma}{M} + \boldsymbol{I}\right| \tag{7}$$

$$= \log_2\left|\boldsymbol{U}_A\boldsymbol{D}_A\boldsymbol{U}_A^H\boldsymbol{U}_W\boldsymbol{D}_W\boldsymbol{U}_W^H\frac{\gamma}{M} + \boldsymbol{I}\right| \tag{8}$$

where $\boldsymbol{D}_A$ and $\boldsymbol{D}_W$ are the diagonal eigenvalue matrices

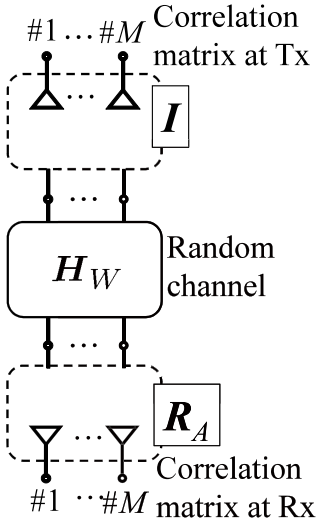

Fig. 2 Block diagram of channel model.

for the correlation matrices calculated from antenna S-parameter and iid channel matrices, respectively, and they are represented by $\boldsymbol{D}_A = \mathrm{diag}[\lambda_{A1}, \ldots, \lambda_{AM}]$ and $\boldsymbol{D}_W = \mathrm{diag}[\lambda_{W1}, \ldots, \lambda_{WM}]$. $\boldsymbol{U}_A$ and $\boldsymbol{U}_W$ are the eigenvector matrices corresponding to $\boldsymbol{D}_A$ and $\boldsymbol{D}_W$, respectively, and are unitary matrices. From (8), it can be seen that the $\boldsymbol{D}_A$ is implicitly multiplied by $\boldsymbol{D}_W$, i.e. their eigenvalues are transformed by unitary matrix. For this case, the upper and lower boundary of (8) can be calculated by,

$$C_{high} = \sum_{i=1}^{M} \log_2(1 + \lambda_{Ai}\lambda_{Wi}\gamma/M) \tag{9}$$

$$C_{low} = \sum_{i=1}^{M} \log_2(1 + \lambda_{Ai}\lambda_{W(M+1-i)}\gamma/M) \tag{10}$$

where the relation, $C_{low} < C < C_{high}$, is satisfied [17]. $\boldsymbol{U}_A^H\boldsymbol{U}_W$ in (8) is a unitary matrix representing the interaction between the modes of the antenna and propagation, and the resulting capacity varies depending on the trial. (9)–(10) indicate the upper bound capacity is realized when the eigenvalue orderings of the antenna and propagation modes agree, and the lower bound is realized when the eigenvalue orderings of them are in reverse.

In (9)–(10), the eigenvalue of the propagation mode, λ_{Wi}, is an instantaneous value, and varies depending on the trial, too. Since the objective of this study is the estimation of the mean channel capacity without Monte Carlo simulation, the knowledge of the statistic eigenvalue distribution is desirable rather than the instantaneous values. This study uses mean eigenvalue distribution of the random channel, which is numerically calculated in advance. Therefore, (9)–(10) corresponding to mean eigenvalue distributions are approximated as,

$$\overline{C_{high}} \simeq \sum_{i=1}^{M} \log_2(1 + \lambda_{Ai}\overline{\lambda_{Wi}}\gamma/M). \tag{11}$$

$$\overline{C_{low}} \simeq \sum_{i=1}^{M} \log_2(1 + \lambda_{Ai}\overline{\lambda_{W(M+1-i)}}\gamma/M). \tag{12}$$

Note that the channel capacity consists of the logarithm of the linear function of the eigenvalues. This means geometric means of the eigenvalues, $\overline{\lambda_{Wi}}$, will yield better accuracy rather than arithmetic means ($\because \frac{1}{N}(\log x_1 + \log x_2 \cdots + \log x_N) = \log(x_1 x_2 \cdots x_N)^{1/N}$). Finally, we assume the mean capacity becomes around the middle of $\overline{C_{high}}$ and $\overline{C_{low}}$, and is expressed as,

$$C \simeq \frac{\overline{C_{low}} + \overline{C_{high}}}{2}. \tag{13}$$

As described above, the mean channel capacity can be easily calculated from S-parameters of antenna and SNR.

Figure 3 is the flowchart of the mean capacity measurement of MIMO antenna, where the scheme differences among the existing and proposed methods are shown. Figure 3(a) represents a direct method, where the MIMO channels of the fabricated antenna are directly measured by the MIMO channel sounder, and this method has been well used in many studies [11]–[13], [18], [19]. Although the use of the existing wireless systems is effective in measuring the data-rate, the results contain non-antenna oriented factors, such as other RF device characteristics, modulation schemes, the control of the other layer in the system, and so on. In the scheme (a), the channel sounder is costly and takes a long time for measuring many channels because the antennas need to be placed at the various locations and orientations. Figure 3(b) shows the hybrid method, where only the antennas are fabricated and channels are computationally generated [2], [16], [20]. This scheme does not need either the expensive channel sounder or exhausting channel measurements. Nevertheless, the MIMO channel needs to be adequately modeled for evaluating the MIMO antennas. Furthermore, the mean channel capacity cannot be straightforwardly calculated even though the antenna characteristics of the MIMO antenna are constant and deterministic. Therefore, we still need several steps for obtaining the mean channel capacity. Figure 3(c) shows the scheme of the proposed approach. It is obvious that the proposed method needs only a few steps if our interest is the mean channel capacity. Although this idea has been already presented by the authors [15], the previous method has a problem in accuracy. If the accuracy is significantly improved, the proposed method will be more practical than the previous method.

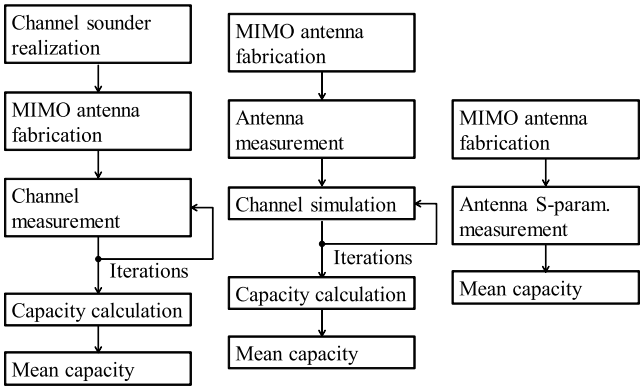

(a) Direct method (b) Hybrid method (c) Proposed method

Fig. 3 Flowchart comparison of the various measurement methods of MIMO antenna capacity.

3. Simulation

Figure 4 shows the simulated MIMO array model, where M-element uniform linear dipole array is assumed, and d is inter-element spacing. The S-parameter matrix and 3D complex radiation patterns of the MIMO array are calculated by Moment Method. Here, each radiation pattern corresponding to each feed port is calculated by terminating other ports with 50 Ω loads. In order to evaluate the accuracy of the proposed method, two types of Monte Carlo simulations are used. First one uses Kronecker model, which is defined by (4). This model uses Gaussian random matri-

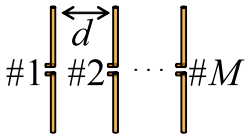

Fig. 4 Simulated antenna model.

ces, where each of their elements has zero-mean complex Gaussian distribution with $\sigma^2 = 1$ (σ^2: variance). For this scheme, the correlation matrix calculated from S-parameter matrix of the antenna is used. This means, the error caused by the ohmic loss cannot be evaluated correctly. Second one is a geometry-based channel model (GCM) [16], which uses complex radiation patterns and geometrically defined rays that go through the randomly distributed scatterers at the transmitting and receiving sides. The distribution of the instantaneous amplitude of the channel corresponds to Gaussian distribution, and the variance of the channel is normalized to 1 when the omni-directional antenna is used at both the transmitting and receiving sides. That is, the entire radiation characteristics including the efficiency of the antennas are taken into account, whereas the Kronecker model described above cannot consider the ohmic loss. Also, 3D-uniform path distribution with no direct path is assumed, and the number of the paths is set to 100. To uncorrelated transmitting side, the ideal omni-directional antennas with sufficiently wide inter-element spacing (10 wavelengths) are used. For both Monte Carlo simulations, the number of the simulation trials is set to 1000.

In the following discussion, the Kronecker model is used only for the verification of the intermediate results of the proposed method. Also, it must be noted that these Monte Carlo simulations are just for the verification of the proposed method, and not used in the proposed method.

To verify the assumption that the mean capacity is approximated by (13), the upper and lower bounds calculated by (9) and (10) are evaluated by the Monte Carlo simulation based on the Kronecker model. Figure 5 shows cumulative distribution function (CDF) of C_{high} and C_{low}, where the values are normalized by the instantaneous capacity, C, i.e. straightforwardly calculated by (5). In this simulation, the number of the antenna elements is set to $M = 4$, and SNR is 20 dB. The element spacings for Fig. 5(a) and (b) are $d = 0.2\lambda_0$, $1.0\lambda_0$ (λ_0: wavelength in vacuum), respectively. From this result, it can be seen that C is just middle of the distributions of the upper and lower bounds. This result supports (13) well approximate mean channel capacity. Also, the result for $d = 1.0\lambda_0$ indicates that C_{high} and C_{low} are quite close. In this case, the antennas are sufficiently separated, and the difference in $\lambda_{A1} \sim \lambda_{AM}$ is small. This means (9) and (10) yield almost similar values.

Figure 6 shows $E[C_{high}]$ and $E[C_{low}]$ versus d, where the Monte Carlo simulation based on the Kronecker model was used. $(E[C_{high}] + E[C_{low}])/2$ and actual mean capacity, $E[C]$, calculated by (5) are also shown. Where, the operation $E[\cdot]$ represents ensemble average. It can be seen that

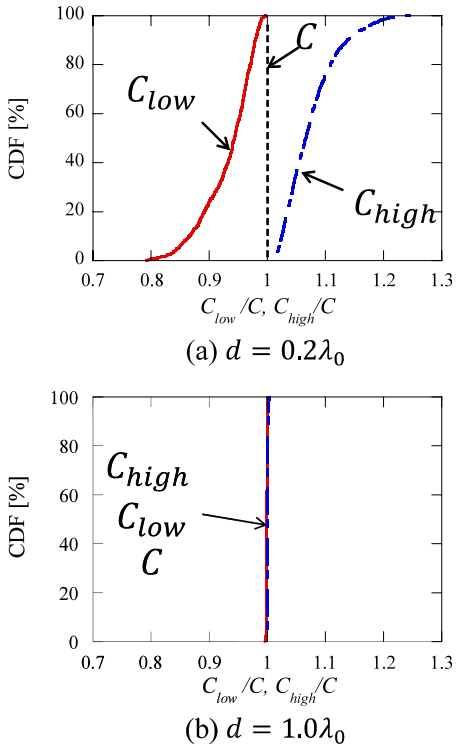

Fig. 5 CDF of capacity upper bound (C_{high}) and lower bound (C_{low}) for $M = 4$.

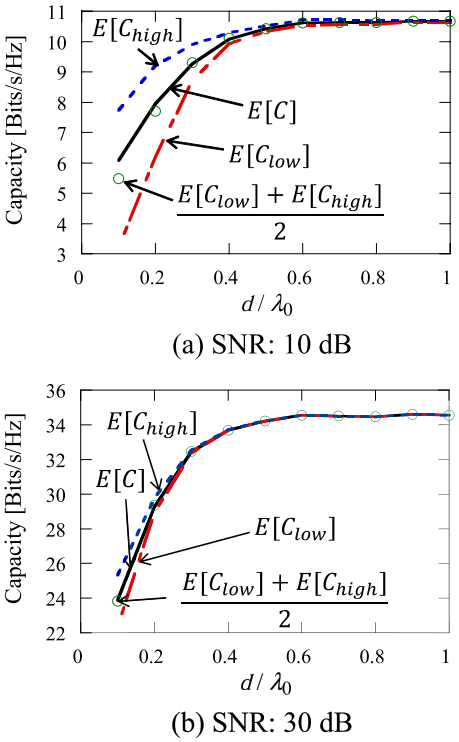

Fig. 6 Mean channel capacity versus element spacing, d.

$E[C]$ is in almost middle of $E[C_{low}]$ and $E[C_{high}]$. Similarly to Fig. 5, $E[C_{high}]$ and $E[C_{low}]$ approach when the antenna spacing, d, becomes large. Also, it can be seen that

Table 1 Eigenvalue table: geometric means of eigenvalues (λ_{Wi}).

Index of eigenvalues, i \ Number of antennas, M	2	3	4	5	6	7	8
1	3.05	6.11	9.39	12.79	16.28	19.84	23.42
2	0.28	1.89	4.16	6.77	9.59	12.56	15.64
3	–	0.19	1.38	3.21	5.40	7.84	10.45
4	–	–	0.14	1.09	2.62	4.52	6.68
5	–	–	–	0.11	0.91	2.23	3.90
6	–	–	–	–	0.09	0.78	1.94
7	–	–	–	–	–	0.08	0.68
8	–	–	–	–	–	–	0.07

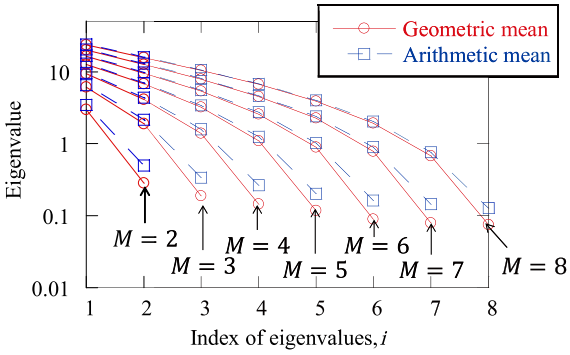

Fig. 7 Arithmetic and geometric means of eigenvalues in Gaussian random matrix.

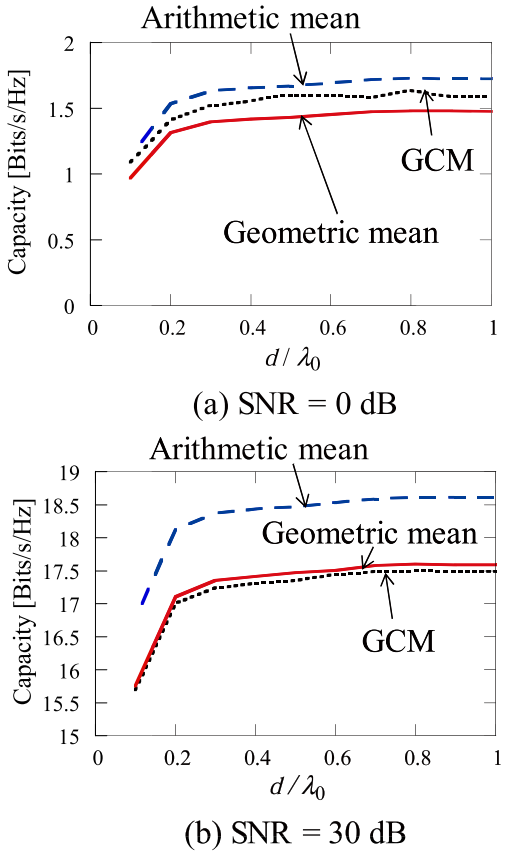

Fig. 8 Capacity versus element spacing, d (M = 2).

$E[C_{high}]$ and $E[C_{low}]$ approach when SNR is high. $E[C]$ and $(E[C_{high}] + E[C_{low}])/2$ well agree even when d and SNR are varied, and this supports the validity of the approximation $E[C] \simeq (E[C_{high}] + E[C_{low}])/2$.

The discussion hereinbefore in this section was based on the Monte Carlo simulation. The important objective of this work is evaluating the mean capacity without Monte Carlo simulation. As mentioned in 2.2, the mean eigenvalues of the random matrix are used for calculating mean capacity. Figure 7 shows arithmetic and geometric means of the eigenvalues, where all of the elements of the random matrix have a Gaussian distribution with zero-mean and unit variance, and mean values are calculated by 10^6 trials. Note that the index number of the eigenvalue is given in descending order of eigenvalue magnitude. It can be seen that the geometric mean value is always smaller than the arithmetic mean, and it is well known as the inequality of arithmetic and geometric means.

In Table 1, the geometric means of the eigenvalues are listed, where they are exact identical to the values shown in Fig 7. This table can be used for calculating the capacity by (11)–(13), and Monte Carlo simulation is no longer needed.

Figure 8 shows the relationship between d and capacity, which is calculated by the proposed equations, (12)–(13), where the number of the elements is $M = 2$. For comparison, the capacity, which is calculated by the Monte Carlo simulation, is shown, too. In the remaining part of the paper, the Monte Carlo simulations are based on GCM. Even though the proposed equation with geometric means of the eigenvalues is slightly lower than the GCM for low SNR case, they well agree for high SNR case. Furthermore, it is found that the results with arithmetic means of the eigenvalues suffer from large errors in capacity.

Figure 9 also shows the relationship between d and capacity when the number of element is $M = 4$. From this result, it can be seen that the capacity equation using arithmetic means of the eigenvalues always overestimates the capacity, and that using geometric ones yields less error regardless of SNR. From the results shown in Figs. 8 and 9, it is found that the proposed equation with geometrical means of the eigenvalues underestimates the capacity only when $SNR = 0$ dB and $M = 2$, whereas all other results overestimate the capacity. Although the reason of this changeover is unclear, this is suspected due to the approximations in (11)–(13). Figure 10 shows the relationship between capac-

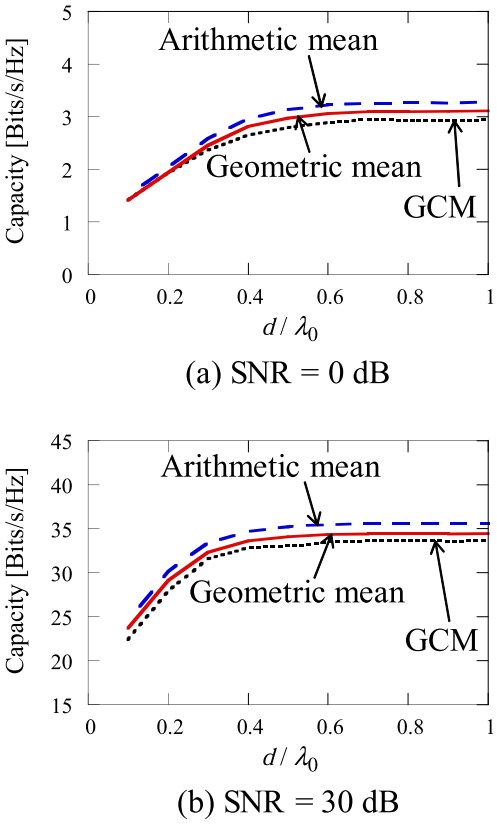

Fig. 9 Capacity versus element spacing, d ($M = 4$).

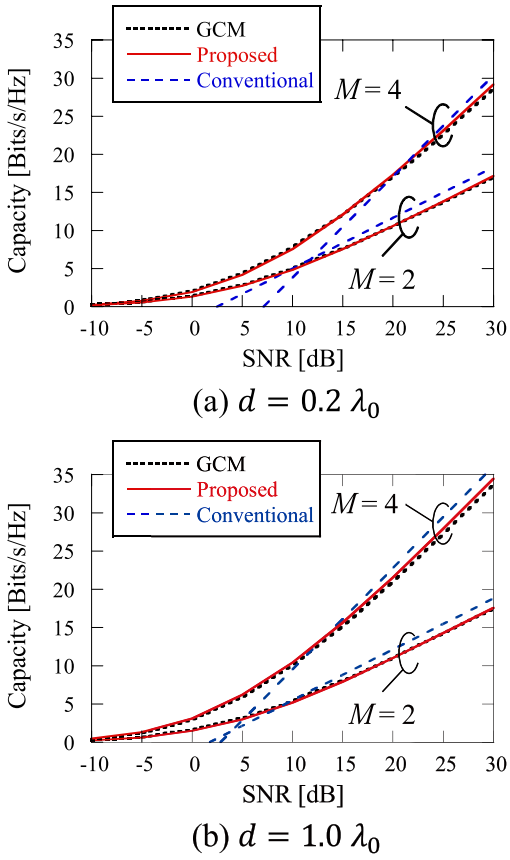

Fig. 10 Capacity versus SNR.

ity and SNR for the cases, $M = 2$ and 4. 'Conventional' represents the capacity calculated by the equation shown in [15], and it suffers from underestimation at low SNR region and overestimation at high SNR region. This is due to the high SNR approximation. Also, it is found that the conventional equation causes large error compared to GCM even in high SNR case. This error comes from the inequality of arithmetic and geometric means [15]. On the other hand, the proposed equation with geometric means of the eigenvalues offers highly accurate capacity independently of the number of the antenna elements, spacing, and SNR.

4. Measurement

The validity of the equation is experimentally assessed in this section. Figure 11(a) and (b) are photos of tested MIMO arrays. The monopole antennas are used for this experiment because the conducting loss is relatively small and the feed cables little affect the radiation characteristics thanks to the ground plane. Two and four element arrays are tested, where a square arrangement is used for four element array. The length of the monopole is around quarter wavelength in vacuum and the size of the ground plane is $1.62\lambda_0 \times 1.62\lambda_0$ for both arrays. The operation frequency for both arrays is 2.4 GHz.

Figure 12(a) and (b) show the capacity as a function of antenna spacing, d. The capacity of the proposed equation is calculated using S-parameter matrix measured by vector

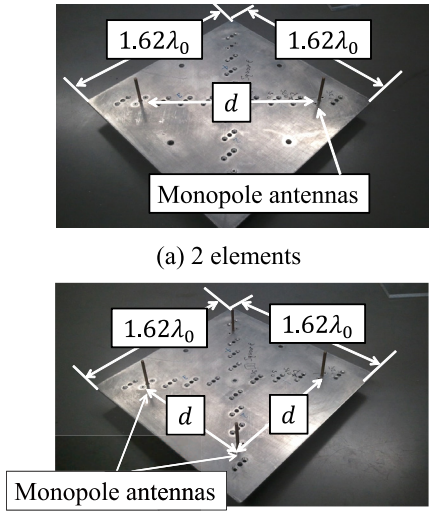

Fig. 11 Measured monopole array.

network analyzer. The results shown by 'GCM' are calculated by geometry-based channel model using measured 3D complex radiation patterns, and all of the channel parameters are identical to that in Sect. 3. It can be seen that almost constant channel capacity is obtained for $M = 2$ and this tendency agrees with that in Fig. 8 ($d > 0.35\lambda_0$). This is

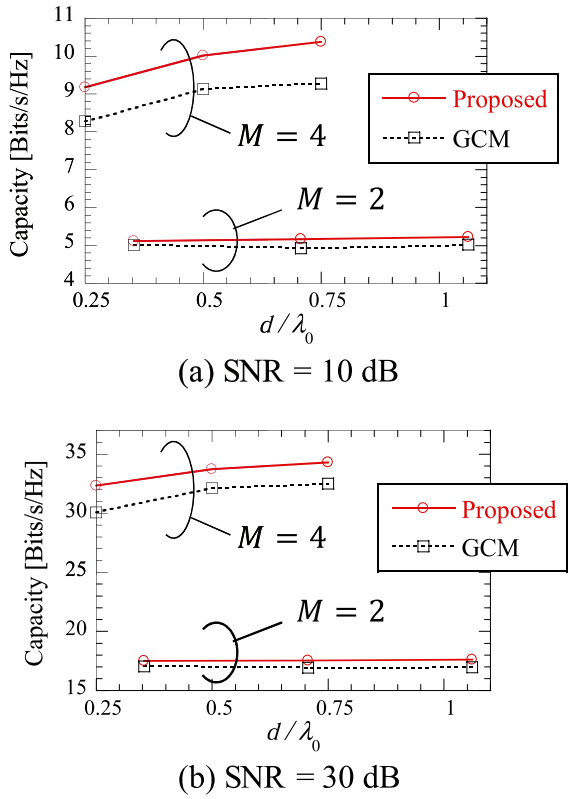

Fig. 12 Capacity versus d (measurement).

because the mutual coupling is too small to affect the capacity for this case. On the other hand, the capacity for $M = 4$ is degraded when d is small because the square array yields mutual coupling higher than linear 2 element array ($M = 2$) does. It can be seen that the proposed method slightly overestimates the channel capacity. To identify the reason of this discrepancy, the radiation efficiency is evaluated using 3D radiation patterns of the monopole array, and it is found that the radiation efficiency of tested array is about 93 $\sim$ 99%. Therefore, it is considered the ohmic loss causes error in this equation because 100% radiation efficiency is assumed for derivation. Nevertheless, the channel capacity is estimated within 12% error even for low SNR case (SNR=10 dB). Since the error is less than 9% for high SNR case (SNR = 30 dB), the accuracy of this equation is about 9% $\sim$ 12% for this experiment.

Figure 13 shows the relationship between the capacity and SNR. It can be seen that the results with the proposed equation well agree with the GCM results regardless of SNR. From this result it is found that the proposed equation well estimates the capacity even when SNR is low.

5. Conclusion

This paper has proposed an equation for mean channel capacity that uses only the S-parameter and SNR. This method uses the eigenvalue table of the correlation matrix, which is calculated only from S-parameter matrix of MIMO antenna.

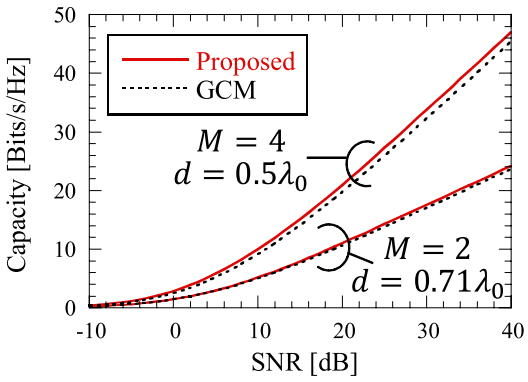

Fig. 13 Capacity versus SNR (measurement).

Also, the equation uses mean eigenvalue distribution of random iid channel, which can be calculated in advance of the evaluation. The proposed equation is valid only when the following conditions are assumed:

- same number of antennas at both transmitting and receiving sides
- no ohmic loss
- 3D uniform Rayleigh environment

The accuracy of the proposed equation was evaluated numerically and experimentally. From the numerical analysis, it is found that the geometric means of eigenvalues give more accurate results than the arithmetic ones. The experiment results showed that the proposed equation offers the mean channel capacity within 12% error regardless of the SNR. These results indicate that the proposed equation is quite convenient to calculate the mean channel capacity since it does not need Monte Carlo simulations of MIMO channel, which has prevented the direct evaluation of MIMO antennas.

Acknowledgements

This research was partially supported by JSPS KAKENHI (25709030).

References

[1] J.W. Wallace and M.A. Jensen, "Mutual coupling in MIMO wireless systems: A rigorous network theory analysis," IEEE Trans. Wireless Commun., vol.3, no.4, pp.1317–1325, July 2004.
[2] B.K. Lau, J.B. Andersen, G. Kristensson, and A.F. Molisch, "Impact of matching network on bandwidth of compact antenna arrays," IEEE Trans. Antennas Propag., vol.54, no.11, pp.3225–3238, Nov. 2006.
[3] D.W. Browne, M. Manteghi, M.P. Fitz, and Y. Rahmat-Samii, "Experiments with compact antenna arrays for MIMO radio communications," IEEE Trans. Antennas Propag., vol.54, no.11, pp.3239–3250, Nov. 2006.
[4] P.-S. Kildal and K. Rosengren, "Correlation and capacity of MIMO systems and mutual coupling, radiation efficiency, and diversity gain of their antennas: Simulations and measurements in a reverberation chamber," IEEE Commun. Mag., vol.42, no.12, pp.104–112, Dec. 2004.
[5] T. Taga, "Analysis for mean effective gain of mobile antennas in

land mobile radio environments," IEEE Trans. Veh. Technol., vol.39, no.2, pp.117–131, May 1990.
[6] K. Ogawa and T. Matsuyoshi, "An analysis of the performance of a handset diversity antenna influenced by head, hand, and shoulder effects at 900 MHz Part I — Effective gain characteristics," IEEE Trans. Veh. Technol., vol.50, no.3, pp.830–844, May 2001.
[7] K. Ogawa, T. Matsuyoshi, and K. Monma, "An analysis of the performance of a handset diversity antenna influenced by head, hand, and shoulder effects at 900 MHz Part II — Correlation characteristics," IEEE Trans. Veh. Technol., vol.50, no.3, pp.845–853, May 2001.
[8] Y. Okano and K. Cho, "Antenna measurement system for mobile terminals," NTT DoCoMo Technical J., vol.9, no.2, pp.43–50, 2007.
[9] L. Duchesne, P. Garreau, N. Robic, A. Gandois, P.O. Iversen, and G. Barone, "Compact multi-probe antenna test station for rapid testing of antennas and wireless terminals," Technical Seminar on Antenna Measurements and SAR (AMS 2004), pp.101–105, Jan. 2004.
[10] S. Blanch, J. Romeu, and I. Corbella, "Exact representation of antenna system diversity performance from input parameter description," Electron. Lett., vol.39, no.9, pp.705–707, May 2003.
[11] J.W. Wallace, M.A. Jensen, A.L. Swindlehurst, and B.D. Jeffs, "Experimental characterization of the MIMO wireless channel: Data acquisition and analysis," IEEE Trans. Wireless Commun., vol.2, no.2, pp.335–343, March 2003.
[12] D.W. Browne, M. Manteghi, M.P. Fitz, and Y. Rahmat-Samii, "Experiments with compact antenna arrays for MIMO radio communications," IEEE Trans. Antennas Propag., vol.54, no.11, pp.3239–3250, Nov. 2006.
[13] N. Honma, K. Nishimori, R. Kudo, Y. Takatori, T. Hiraguri, and M. Mizoguchi, "A stochastic approach to design MIMO antenna with parasitic elements based on propagation characteristics," IEICE Trans. Commun., vol.E93-B, no.10, pp.2578–2585, Oct. 2010.
[14] N. Honma, Y. Tsunekawa, and K. Ogawa, "Evaluation of capacity equation only based on S-parameter for realistic MIMO antenna," 2013 IEEE Antennas and Propagation Society International Symposium (APSURSI), pp.548–549, 2013.
[15] N. Honma, H. Sato, K. Ogawa, and Y. Tsunekawa, "Accuracy of MIMO channel capacity equation based only on S-parameters of MIMO antenna," Antennas Wirel. Propag. Lett., vol.14, pp.1250–1253, June 2015.
[16] A.F. Molisch, "A generic model for MIMO wireless propagation channels in macro- and microcells," IEEE Trans. Signal Process., vol.52, no.1, pp.61–71, Jan. 2004.
[17] M. Fiedler, "Bounds for the determinant of the sum of hermitian matrices," Proc. Amer. Math. Soc., vol.30, no.1, pp.27–27, 1971.
[18] J.P. Kermoal, L. Schumacher, K.I. Pedersen, P.E. Mogensen, and F. Frederiksen, "A stochastic MIMO radio channel model with experimental validation," IEEE J. Sel. Areas. Commun., vol.20, no.6, pp.1211–1226, Aug. 2002.
[19] V. Jungnickel, V. Pohl, and C.V. Helmolt, "Capacity of MIMO systems with closely spaced antennas," IEEE Commun. Lett., vol.7, no.8, pp.361–363, Aug. 2003.
[20] Y. Okano and K. Cho, "Monopole antenna array arrangement for card-type mobile terminal," Proc. 2004 IEEE Radio and Wireless Conference, pp.415–418, 2004.

Appendix: Derivations of (7) and (8)

In this appendix, the derivations of (7) and (8) from (6) are detailed. The eigenvalue decomposition of the correlation matrix of (3) is expressed as,

$$\boldsymbol{R}_A = \boldsymbol{U}_A \boldsymbol{D}_A \boldsymbol{U}_A^H, \tag{A·1}$$

where $\boldsymbol{U}_A (\in \mathbb{C}^{M\times M})$ and $\boldsymbol{D}_A (\in \mathbb{C}^{M\times M})$ are the eigenvector matrix and diagonal eigenvalue matrix, respectively. Since $\boldsymbol{R}_A$ is Hermitian matrix, all eigenvalues are real. The eigenvalues are positive or zero because they represent the reception power corresponding to the eigenmodes. The square root of (A·1) is,

$$\boldsymbol{R}_A^{1/2} = \boldsymbol{U}_A \boldsymbol{D}_A^{1/2} \boldsymbol{U}_A^H, \tag{A·2}$$

because

$$\begin{aligned} \boldsymbol{R}_A^{1/2}\boldsymbol{R}_A^{1/2} &= \boldsymbol{U}_A \boldsymbol{D}_A^{1/2} \boldsymbol{U}_A^H \boldsymbol{U}_A \boldsymbol{D}_A^{1/2} \boldsymbol{U}_A^H & \text{(A·3)}\\ &= \boldsymbol{U}_A \boldsymbol{D}_A \boldsymbol{U}_A^H & \text{(A·4)}\\ &= \boldsymbol{R}_A. & \text{(A·5)} \end{aligned}$$

Also,

$$\begin{aligned} \boldsymbol{R}_A^{1/2H}\boldsymbol{R}_A^{1/2} &= (\boldsymbol{U}_A \boldsymbol{D}_A^{1/2} \boldsymbol{U}_A^H)^H \boldsymbol{U}_A \boldsymbol{D}_A^{1/2} \boldsymbol{U}_A^H & \text{(A·6)}\\ &= \boldsymbol{U}_A \boldsymbol{D}_A \boldsymbol{U}_A^H & \text{(A·7)}\\ &= \boldsymbol{R}_A & \text{(A·8)} \end{aligned}$$

is satisfied. These relations are used in the following part of the derivation.

Now, the part of the determinant in (6) is considered for simplicity, and can be rewritten as,

$$\begin{aligned} &\left|\boldsymbol{R}_A^{1/2}\boldsymbol{H}_W\boldsymbol{H}_W^H\boldsymbol{R}_A^{1/2H}\frac{\gamma}{M} + \boldsymbol{I}\right| \\ &= \left|\boldsymbol{R}_A^{1/2}\right|\left|\boldsymbol{H}_W\boldsymbol{H}_W^H\frac{\gamma}{M} + \boldsymbol{R}_A^{-1/2}\boldsymbol{R}_A^{-1/2H}\right|\left|\boldsymbol{R}_A^{1/2H}\right| \\ &= \left|\boldsymbol{R}_A^{1/2}\right|\left|\boldsymbol{H}_W\boldsymbol{H}_W^H\frac{\gamma}{M} + \boldsymbol{R}_A^{-1}\right|\left|\boldsymbol{R}_A^{1/2H}\right| \\ &= \left|\boldsymbol{R}_A^{1/2}\right|\left|\boldsymbol{R}_A^{1/2H}\right|\left|\boldsymbol{R}_A^{-1}\right|\left|\boldsymbol{R}_A\boldsymbol{H}_W\boldsymbol{H}_W^H\frac{\gamma}{M} + \boldsymbol{I}\right| \\ &= \left|\boldsymbol{R}_A\boldsymbol{H}_W\boldsymbol{H}_W^H\frac{\gamma}{M} + \boldsymbol{I}\right|. \end{aligned} \tag{A·9}$$

As shown the derivation above, (A·9) validates the transformation from (6) to (7). Finally, $\boldsymbol{H}_W\boldsymbol{H}_W^H$ is replaced by its eigenvalue decomposition:

$$\boldsymbol{H}_W\boldsymbol{H}_W^H = \boldsymbol{U}_W\boldsymbol{D}_W\boldsymbol{U}_W^H, \tag{A·10}$$

where $\boldsymbol{U}_W (\in \mathbb{C}^{M\times M})$ and $\boldsymbol{D}_W (\in \mathbb{C}^{M\times M})$ are the eigenvector matrix and diagonal eigenvalue matrix, respectively, and we obtain

$$\begin{aligned} &\left|\boldsymbol{R}_A\boldsymbol{H}_W\boldsymbol{H}_W^H\frac{\gamma}{M} + \boldsymbol{I}\right| \\ &= \left|\boldsymbol{U}_A\boldsymbol{D}_A\boldsymbol{U}_A^H\boldsymbol{U}_W\boldsymbol{D}_W\boldsymbol{U}_W^H\frac{\gamma}{M} + \boldsymbol{I}\right|, \end{aligned} \tag{A·11}$$

which supports the validity of (8).

Naoki Honma received the B.E., M.E., and Ph.D. degrees in electrical engineering from Tohoku University, Sendai, Japan in 1996, 1998, and 2005, respectively. In 1998, he joined the NTT Radio Communication Systems Laboratories, Nippon Telegraph and Telephone Corporation (NTT), in Japan. He is now working for Iwate University. He received the Young Engineers Award from the IEICE of Japan in 2003, the APMC Best Paper Award in 2003, the Best Paper Award of IEICE Communication Society in 2006, and 2014 Asia-Pacific Microwave Conference Prize in 2014, respectively. His current research interest is MIMO system and its applications. He is a member of IEEE.

Kentaro Murata received the B.E. and M.E. degrees in electrical and electronics engineering from Iwate University, Morioka, Japan in 2011 and 2014, respectively. He is currently working toward the Ph.D. degree with Graduate School of Science and Engineering, National Defense Academy of Japan, Yokosuka, Japan. His current research interests include feeding methods for multiple-input-multiple-output antenna systems.

Hiroshi Sato was born in Tokyo, Japan, on August 2, 1975. He received B.S. and M.S. degree in electrical engineering from Tokyo City University, Japan, in 1998 and 2000, respectively. He is currently researching for his Ph.D. degree in Graduate School of Engineering from Chiba University, Japan. From 2004 to 2012, he has been with Panasonic Mobile Communication Co., Ltd., Yokosuka, Japan. And is currently a leader of the R&D project for mobile phone antennas in Panasonic System Networks Co., Ltd, Yokohama, Japan. His research interests include small antenna, MIMO antenna and decoupling technique. He was the recipient of the Best Paper Award from the Institute of Electronics, Information and Communication Engineers (IEICE) Transactions of Japan in 2012. He is a member of IEEE.

Koichi Ogawa was born in Kyoto on May 28, 1955. He received his B.S. and M.S. degrees in electrical engineering from Shizuoka University in 1979 and 1981, respectively. He received the Ph.D. degree in electrical engineering from the Tokyo Institute of Technology, Tokyo, Japan, in 2000. He joined Matsushita Electric Industrial Co., Ltd., Osaka, Japan, in 1981. He is currently a Professor with Toyama University, Toyama, Japan. His research interests include compact antennas, diversity, adaptive, and MIMO antennas for mobile communication systems, and electromagnetic interaction between antennas and the human body. His research also includes millimeter-wave circuitry and other related areas of radio propagation. Dr. Ogawa was the recipient of the OHM Technology Award from the Promotion Foundation for Electrical Science and Engineering in 1990, based on his accomplishments and contributions to the millimeter-wave technologies. He was also the recipient of the TELECOM System Technology Award from the Telecommunications Advancement Foundation (TAF) in 2001, based on his accomplishments and contributions to portable handset antenna technologies, and the Best Paper Award from the Institute of Electronics, Information and Communication Engineers (IEICE) Transactions of Japan in 2009 and 2012. He is a Senior Member of the IEEE and is listed in *Who's Who in the World*. He is currently the Chair of the IEEE AP-S Nagoya Chapter.

Yoshitaka Tsunekawa received the B.E. degree from Iwate University, Morioka, Japan, in 1980 and the M.E. and the Doctor of Engineering degrees from Tohoku University, Sendai, Japan, in 1983 and 1993, respectively. Since 1983, he has been with the Faculty of Engineering, Iwate University, where he is now a professor at the Department of Electrical Engineering and Computer Science. His current research interests include digital signal processing and digital control. He is a member of the Institute of Electronics, Information and Communication Engineers of Japan, and IEEE.